A RIGOROUS ANALYSIS OF DIELECTRIC RING RESONATORS LOADED IN WAVEGUIDE OR MICROSTRIP LINE STRUCTURE

Seng-Woon Chen† and Kawthar A. Zaki‡

† COMSAT Systems Division, Clarksburg, MD 20871

‡ Electrical Engineering Department, University of Maryland, College Park, MD 20742

Abstract— A rigorous mode matching technique is used to analyze the dielectric ring resonators loaded in waveguide or microstrip line structure. Variations of the resonant frequencies for several lowest order modes with the structures' parameters are presented. Analysis shows that increasing the inner concentric hole's diameter of a dielectric ring resonator up to 25% of its outside diameter changes the TE_{01} mode resonant frequency by less than 1%, however, increases the spurious mode free region by greater than 80% compared with the dielectric rod resonator. Two-dimensional electric and magnetic field line patterns and three-dimensional field intensity distributions of the ring resonator are plotted, which provide valuable information on mode excitation, coupling, and suppression. Coupling between two dielectric ring resonators loaded in a metallic cavity are analyzed for application in the filter design. Experimental results are presented and shows excellent agreement with the analysis solutions within 1%.

Introduction

The last two decades have witnessed the increasing application of dielectric resonators in a variety of microwave components and subsystems, such as filters [1] and oscillators [2], because of their superior characteristics of high Q, low manufacturing cost, temperature stability, miniaturization, and compatibility with microwave integrated circuits (MICs) and monolithic microwave integrated circuits (MMICs).

The circular cylindrical dielectric resonators have been widely used due to their simple geometry, commercial availability, and easy to be analyzed. In practical applications, some low loss and low permittivity material, such as microwave foam or quartz crystal, is used to support the dielectric resonators. However, the support is not stable enough in stringent vibrational environments. To enhance mechanical stability, the ring-shaped dielectric resonators have been used such that an additional supporting rod can pass through the inner hole to provide stability. The dielectric ring resonators give one more degree of freedom (dimension of the inner hole) than rod resonator in determining the dimensions of the resonator for a fixed resonant frequency and provide wider spurious mode free range. Another advantage of the dielectric ring resonators is to provide reasonable dimension at a high frequency range, such as K- and Ka-bands. For a dielectric resonator rod, the dimension of the resonator is reduced by a factor of about $\sqrt{\epsilon_r}$, where ϵ_r is the relative dielectric constant of the dielectric resonator, in comparison with an empty metallic cavity. At high frequency, 30 GHz for example, the diameter of the dielectric resonator resonating at $TE_{01\delta}$ mode will be only $\sim 0.080''$ for $\epsilon_r = \sim 30$ and aspect ratio = 2.5. This small size may cause difficulties in manufacturing, tolerance and effective coupling to a transmission line. One possible approach to relieve this problem is to use a dielectric ring resonator.

A rigorous analysis of dielectric ring resonators has been reported by Kobayashi [3], where the resonators were assumed to be loaded inside a conducting cavity both radially and longitudinally. Coupling between two $TE_{01\delta}$ mode dielectric ring resonators was presented and applied in a Chebyshev filter design by the same author in [4]. In this paper, a mode matching technique is applied to analyze the resonant frequencies and field distributions for all possible resonant modes of the asymmetric dielectric loaded ring resonator as shown in Fig.1(a), and the ring resonator placed on the substrate of a microstrip line structure shown in Fig.1(c). Coupling between two dielectric ring resonators with both TE and HE mode excitations are also presented. These results are helpful to the design of direct-coupled-resonator as well as multiple-coupled-mode filters.

V

Analysis

By mode matching technique [5]-[6], the structure under analysis is partitioned into several subregions in accordance with the spatial and/or material discontinuities. For the structures shown in Fig.1, it is convenient to divide each into three sub-regions denoted by A, B, and C.

Expressing the total transverse electric and magnetic fields in each region as linear combinations of its eigenmode fields, we obtain

CH2870-4/91/0000-0731$01.00 © 1991 IEEE

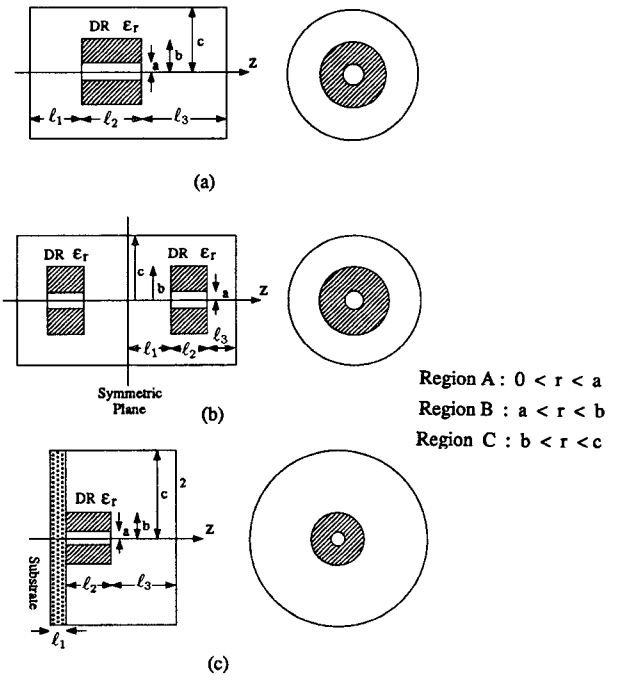

Fig.1 (a) Asymmetric dielectric loaded ring resonator; (b) Double dielectric ring resonator; and (c) Dielectric ring resonator placed on the substrate of a microstrip line structure.

$$\vec{\mathbf{E}}_A(r,\phi,z) = \sum_{i=1}^{\infty} A_i \hat{\mathbf{e}}_{A_i}(\phi,z) g^e_{A_i}(\xi_{A_i} r) \tag{1}$$

$$\vec{\mathbf{H}}_A(r,\phi,z) = \sum_{i=1}^{\infty} A_i \hat{\mathbf{h}}_{A_i}(\phi,z) g^h_{A_i}(\xi_{A_i} r) \tag{2}$$

$$\vec{\mathbf{E}}_B(r,\phi,z) = \sum_{j=1}^{\infty} \hat{\mathbf{e}}_{B_j}(\phi,z) \left[B_j^+ g^e_{B_j^+}(\xi_{B_j} r) + B_j^- g^e_{B_j^-}(\xi_{B_j} r) \right] \tag{3}$$

$$\vec{\mathbf{H}}_B(r,\phi,z) = \sum_{j=1}^{\infty} \hat{\mathbf{h}}_{B_j}(\phi,z) \left[B_j^+ g^h_{B_j^+}(\xi_{B_j} r) + B_j^- g^h_{B_j^-}(\xi_{B_j} r) \right] \tag{4}$$

$$\vec{\mathbf{E}}_C(r,\phi,z) = \sum_{k=1}^{\infty} C_k \hat{\mathbf{e}}_{C_k}(\phi,z) g^e_{C_k}(\xi_{C_k} r) \tag{5}$$

$$\vec{\mathbf{H}}_C(r,\phi,z) = \sum_{k=1}^{\infty} C_k \hat{\mathbf{h}}_{C_k}(\phi,z) g^h_{C_k}(\xi_{C_k} r) \tag{6}$$

where the indices i,j and k should cover all the possible eigenmodes for regions A, B and C; respectively. The field distributions of the eigenmodes in each region as a function of r are represented by $g^q_p(\xi_p r)$, which is a linear combination of Bessel or associated Bessel functions of the first and second kind. By matching the boundary conditions at $r = a$ and $r = b$, appropriate definition of the inner products, and application of the orthogonality property, two set of linear equations are obtained:

$$\sum_{j=1}^{\infty} \left[\lambda_{ij}^{AB^+} B_j^+ + \lambda_{ij}^{AB^-} B_j^- \right] = 0 \ ; \quad \mathrm{i} = 1, 2, \cdots \tag{7}$$

$$\sum_{j=1}^{\infty} \left[\lambda_{ij}^{CB^+} B_j^+ + \lambda_{ij}^{CB^-} B_j^- \right] = 0 \ ; \quad \mathrm{i} = 1, 2, \cdots \tag{8}$$

where

$$\begin{aligned} \lambda_{ij}^{AB^+} &= < \hat{\mathbf{e}}_{B_j}, \hat{\mathbf{h}}_{A_i} > g^e_{B_j^+}(\xi_{B_j} a) g^h_{A_i}(\xi_{A_i} a) \\ &\quad - < \hat{\mathbf{e}}_{A_i}, \hat{\mathbf{h}}_{B_j} > g^h_{B_j^+}(\xi_{B_j} a) g^e_{A_i}(\xi_{A_i} a) \end{aligned} \tag{9}$$

$$\begin{aligned} \lambda_{ij}^{AB^-} &= < \hat{\mathbf{e}}_{B_j}, \hat{\mathbf{h}}_{A_i} > g^e_{B_j^-}(\xi_{B_j} a) g^h_{A_i}(\xi_{A_i} a) \\ &\quad - < \hat{\mathbf{e}}_{A_i}, \hat{\mathbf{h}}_{B_j} > g^h_{B_j^-}(\xi_{B_j} a) g^e_{A_i}(\xi_{A_i} a) \end{aligned} \tag{10}$$

$$\begin{aligned} \lambda_{kj}^{CB^+} &= < \hat{\mathbf{e}}_{B_j}, \hat{\mathbf{h}}_{C_k} > g^e_{B_j^+}(\xi_{B_j} b) g^h_{C_k}(\xi_{C_k} b) \\ &\quad - < \hat{\mathbf{e}}_{C_k}, \hat{\mathbf{h}}_{B_j} > g^h_{B_j^+}(\xi_{B_j} b) g^e_{C_k}(\xi_{C_k} b) \end{aligned} \tag{11}$$

$$\begin{aligned} \lambda_{kj}^{CB^-} &= < \hat{\mathbf{e}}_{B_j}, \hat{\mathbf{h}}_{C_k} > g^e_{B_j^-}(\xi_{B_j} b) g^h_{C_k}(\xi_{C_k} b) \\ &\quad - < \hat{\mathbf{e}}_{C_k}, \hat{\mathbf{h}}_{B_j} > g^h_{B_j^-}(\xi_{B_j} b) g^e_{C_k}(\xi_{C_k} b) \end{aligned} \tag{12}$$

Equation (7) and (8) constitute a homogeneous linear system. In the form of a matrix expression, we have

$$\begin{bmatrix} \tilde{\mathbf{A}}^{AB^+} & \tilde{\mathbf{A}}^{AB^-} \\ \tilde{\mathbf{A}}^{CB^+} & \tilde{\mathbf{A}}^{CB^-} \end{bmatrix} \begin{bmatrix} \tilde{\mathbf{B}}^+ \\ \tilde{\mathbf{B}}^- \end{bmatrix} = \tilde{\mathbf{A}}\mathbf{B} = \mathbf{0} \tag{13}$$

For the existence of nontrivial solutions to the linear system (13), the determinant of the system has to be zero, that is

$$\det \tilde{\mathbf{A}} = 0 \tag{14}$$

The frequencies satisfying the equation (14) are the resonant frequencies of the structure. To solve the characteristic equation numerically using a digital computers, the linear system of infinite order is truncated to a finite order $2N \times 2N$, where N is the number of eigenmodes required to represent the field in each region and match the boundary conditions over the interface. Once the resonant frequency f_0 is obtained, the fields in the resonator structure could be determined by substituting f_0 into equation (13), solving a subsystem of (2N-1)×(2N-1) order for A_i's, B_j's, and C_k's. The total fields in regions A, B and C are then given by equations (1) to (6).

Results

Computer programs have been developed to undertake the numerical analysis of the dielectric ring resonators. Extensive examination for the boundary conditions and convergence have been made to insure the correctness of the numerical results.

$2a = 0.30''$ $2b = 0.842''$ $2c = 1.13''$
$\ell_1 = \ell_3 = 0.564''$ $\ell_2 = 0.112''$ $\epsilon_r = 37.0$

Mode	Computed (GHz)	Measured (GHz)	Error
TE_{01}	4.056	4.070	-0.34%
HE_{11}	4.850	4.827	0.48%
HE_{21}	6.046	6.103	-0.93%
HE_{12}	6.323	6.387	1.00%
TE_{02}	6.803	6.810	0.03%
TM_{01}	7.410	7.501	-1.20%
HE_{22}	8.387	8.383	0.05%
TM_{02}	8.965	8.902	0.71%

Table 1 Comparison of the measured resonant frequencies for the dielectric loaded ring resonator with the computed solutions.

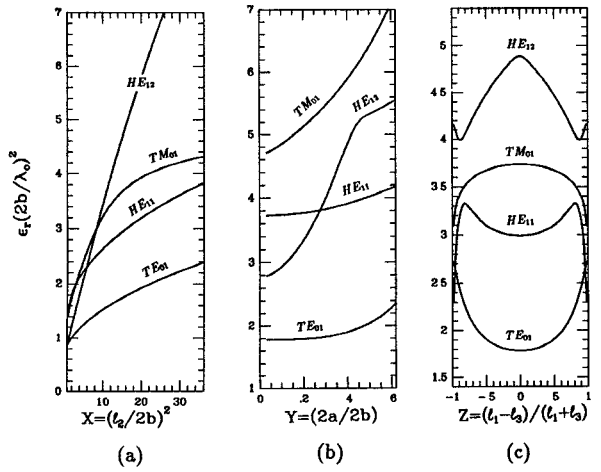

Fig.2 Mode charts of the dielectric loaded ring resonator with resonator's (a) aspect ratio, ($2a = 0.096'', 2b = 0.80'', 2c = 1.60'', \ell_1 = \ell_3 = 0.25'', \epsilon_r = 36.0$), (b) concentric hole's dimension, ($2b = 0.80'', 2c = 1.60'', \ell_1 = \ell_3 = 0.25'', \ell_2 = 0.20'', \epsilon_r = 36.0$), and (c) measure of asymmetry, ($2a = 0.096'', 2b = 0.80'', 2c = 1.60'', \ell_2 = 0.20'', \ell_1 + \ell_3 = 0.50'', \epsilon_r = 36.0$), as the parameters.

Table 1 shows the experimental results of the resonant frequencies for the dielectric loaded ring resonator as show in Fig.1(a). The measured values agree with the computed solution within 1%. Mode chart of the dielectric loaded ring resonator with $X = (2b/\ell_2)^2$, $Y = 2a/2b$, and $Z = (\ell_1 - \ell_3)/(\ell_1 + \ell_3)$ as the parameters are shown in Fig.2(a), Fig.2(b), and Fig.2(c), respectively. Two-dimensional filed lines and three-dimensional field intensity distributions for various modes are plotted and shown in Fig.3. Variation of resonant frequencies and coupling coefficients of a double dielectric ring resonator with the distance between the two resonators is shown in Fig.4(a) and (b). The coupling coefficients are obtained by

$$k = \frac{f_e^2 - f_m^2}{f_e^2 + f_m^2} \tag{15}$$

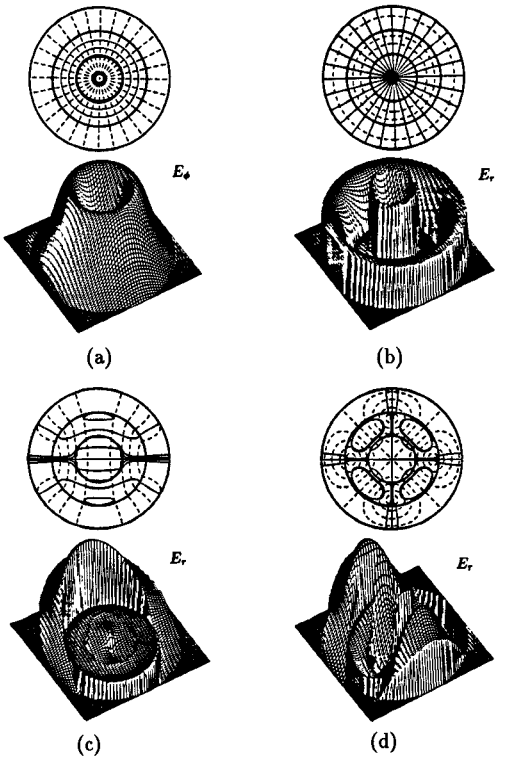

Fig.3 Field lines and 3-d plots of field intensity of the dielectric loaded ring resonator for (a) TE_{01}, (b) TM_{01}, (c) HE_{11} and (d) HE_{21} modes. ($a = 0.2'', b = 0.4'', c = 0.6'', \ell_1 = 0.44'', \ell_2 = 0.24'', \ell_3 = 0.32'', \epsilon_r = 36.0, z = 0.56''$)

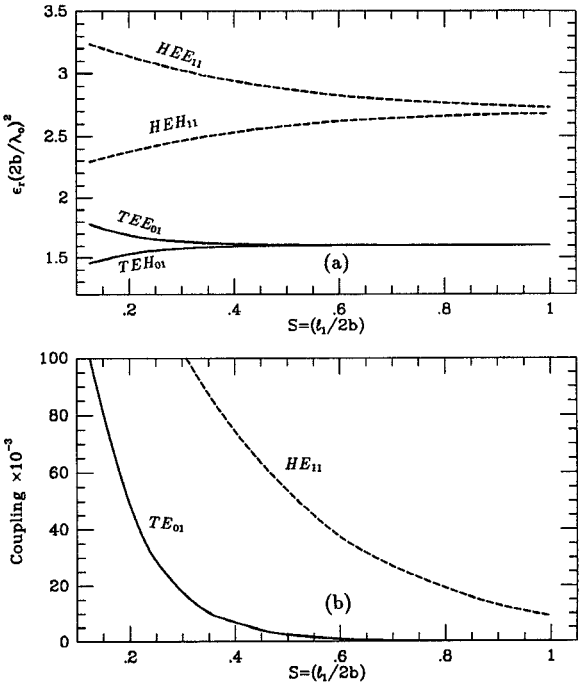

Fig.4 (a) Mode charts and (b) coupling of the double dielectric loaded ring resonator. ($a = 0.1'', b = 0.4'', c = 0.6'', \ell_2 = 0.25'', \ell_3 = 0.4'', \epsilon_r = 36.0$)

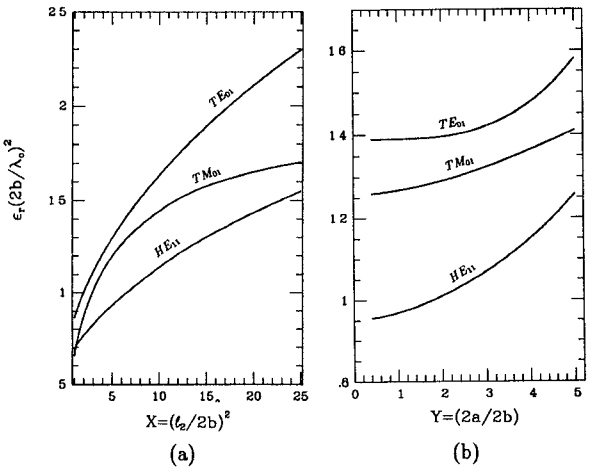

Fig.5 Mode charts of the dielectric ring resonator loaded in a microstrip line structure with resonator's (a) aspect ratio, ($2a = 0.036'', 2b = 0.24'', 2c = 0.60'', \ell_1 = 0.025'', \ell_3 = 0.3'', \epsilon_r = 24.0, \epsilon_{rsub} = 9.9$), (b) concentric hole's dimension, ($2b = 0.24'', 2c = 0.60'', \ell_1 = 0.025'', \ell_2 = 0.096'', \ell_3 = 0.30'', \epsilon_r = 24.0, \epsilon_{rsub} = 9.9$), as the parameters.

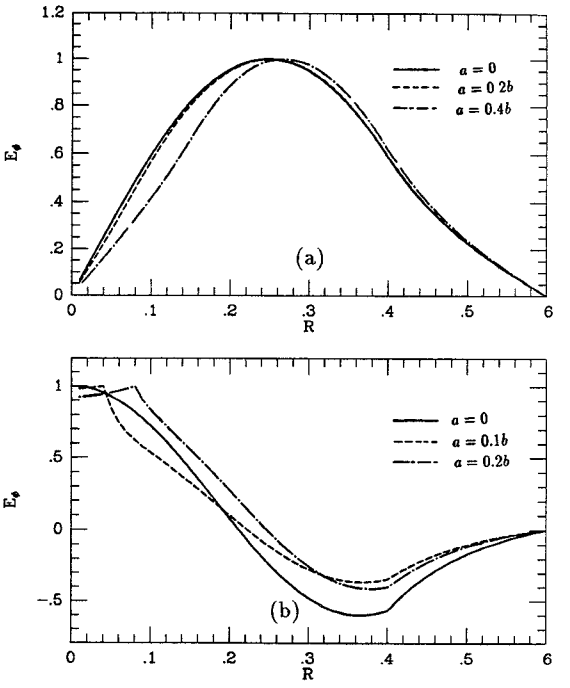

Fig.6 Comparison of field intensity between dielectric ring and disk resonators for (a) TE_{01} and (b) HE_{11} modes. ($b = 0.4''$, $c = 0.6$, $\ell_1 = 0.44''$, $\ell_2 = 0.24''$, $\ell_3 = 0.32''$, $\epsilon_r = 36.0$; $z = 0.56''$).

where f_e and f_m are resonant frequencies assuming PEC and PMC, respectively, in the symmetric plane. With resonator's aspect ratio and dimension of the inner hole as the parameters, mode charts for the dielectric ring resonator place on the Alumina substrate ($\epsilon_r = 9.9$) of a microstrip line structure are shown in Fig.5.

It is shown in Fig.2(b) and Fig.5(b) that increasing the inner concentric hole's diameter of a dielectric ring resonator up to 25% of its outside diameter changes the TE_{01} mode resonant frequency by less than 1%, however, increases the spurious mode free region by greater than 80% compared with the dielectric rod resonator. Fig.6 shows the electric field of the ring resonators with different diameters in the concentric hole. In Fig.6(a), the field distribution of TE_{01} mode ring resonator is little affected by increasing the dimension of the hole up to 20% of the diameter of the resonator. In contrast, a small size of hole causes a considerable modification of the field distribution for HE_{11} mode. These results explain why the resonant frequency of a small hole ring resonator remains close to that of a rod resonator for TE_{01} but not the HE_{11} mode.

Conclusions

Dielectric ring resonators loaded in waveguide cavity and microstrip line structures have been analyzed by a rigorous mode matching technique. Mode charts, field distributions, and coupling among the resonators are presented, which provide valuable information for design of the dielectric ring resonators and their application to microwave filter and oscillator circuits. Experimental verification has been demonstrated and show excellent agreement with the numerical solutions.

REFERENCE

[1] K. A. Zaki, C. Chen and A. E. Atia, "Canonical and longitudinal dual mode dielectric resonator filters without iris," *IEEE Trans. on Microwave Theory and Techniques*, Vol. MTT-35, No. 12, pp. 1130-1135, Dec. 1987.

[2] Seng-Woon Chen et al., "A unified design of dielectric resonator oscillators for telecommunication systems," *Digest of the 1986 IEEE International Microwave Symposium*, pp. 593-596.

[3] Y. Kobayashi and S. Nakayama, "Design charts for shielded dielectric rod and ring resonators," *Digest of the 1986 IEEE International Microwave Symposium*, pp. 241-244.

[4] Y. Kobayashi and M. Minegishi, "Precise design of a bandpass filter using high-Q dielectric ring resonators," *IEEE Trans. on Microwave Theory and Techniques*, Vol. MTT-35, No. 12, pp. 1156-1160, Dec. 1987.

[5] K. A. Zaki and A. E. Atia, "Modes in dielectric loaded waveguides and resonators," *IEEE Trans. on Microwave Theory and Techniques*, Vol. MTT-31, No. 12 , pp. 1039-1045, Dec. 1983.

[6] Seng-Woon Chen, "Analysis and modeling of dielectric loaded resonators, filters and periodic structures," Ph.D dissertation, Electrical Engineering Dept., University of Maryland, College Park, MD 20742.